Cell Reports, Volume *24*

Supplemental Information

Regional Differences in Airway Epithelial Cells Reveal Tradeoff between Defense against Oxidative Stress and Defense against Rhinovirus

Valia T. Mihaylova, Yong Kong, Olga Fedorova, Lokesh Sharma, Charles S. Dela Cruz, Anna Marie Pyle, Akiko Iwasaki, and Ellen F. Foxman

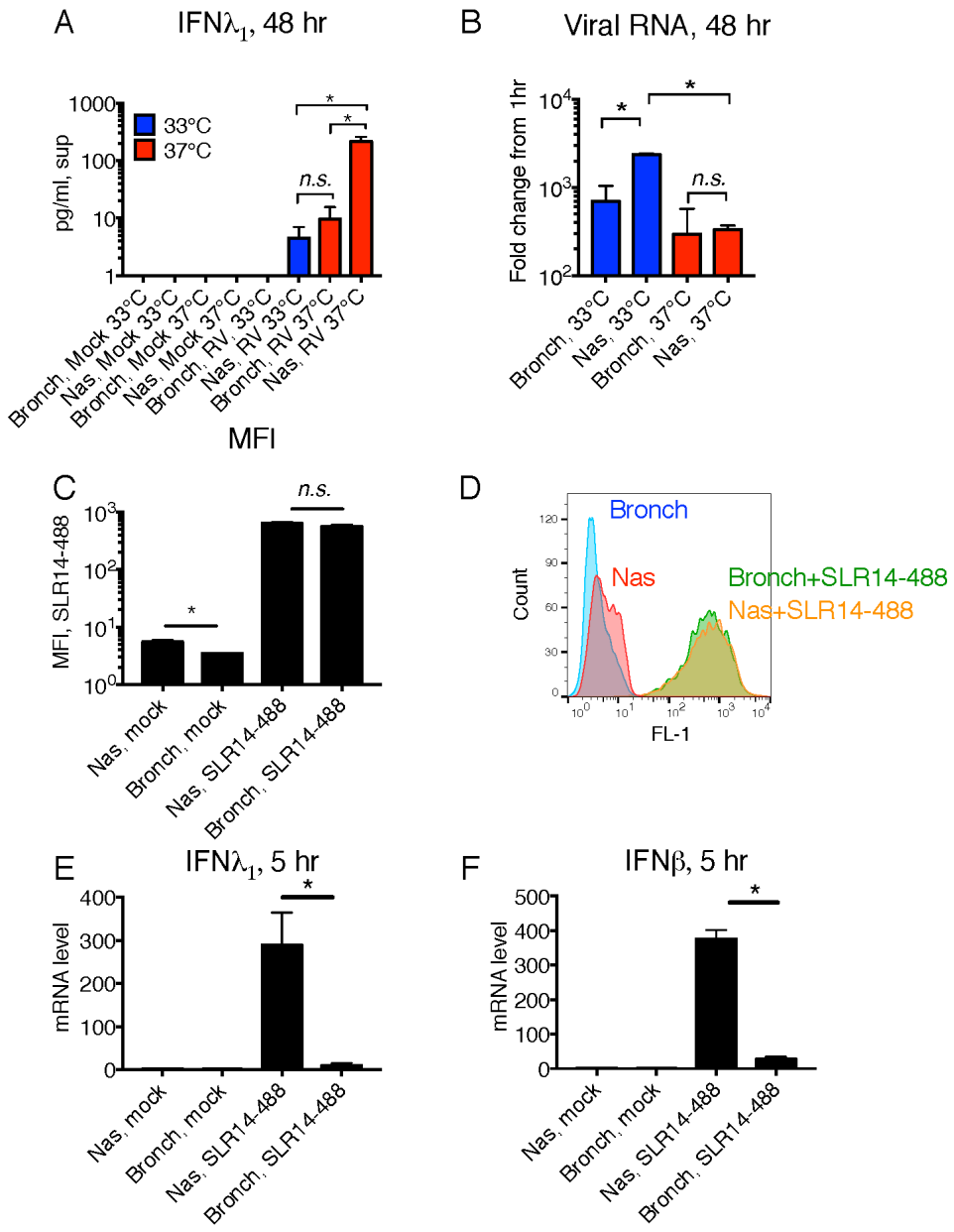

Figure S1. ***Related to Fig 1.*** **Response to RV1B infection or RIG-I stimulation in primary human bronchial and nasal-derived epithelial cells.** Primary human bronchial epithelial cells (bronch) and human nasal epithelial cells (nas) were mock-infected or infected with RV1B, MOI 0.1, then medium was added and cells were incubated for 48 hr at 33°C or 37°C. At this time, supernatants were collected for ELISA and cells were collected to assess viral RNA by RT-qPCR. **(A)** IFNλ1 levels were above the detection limit for only three conditions, as shown. Level of IFNλ1 for nasal cells at 37°C was significantly higher than level in bronchial cells incubated at 37°C or in nasal cells incubated at 33°C (*$p<0.02$). 37°C data only for this experiment is also shown in Figure 1A, however here IFNλ1 level is shown on a LOG_{10} scale to better demonstrate detection of low level of IFNλ1 in two of the conditions. **(B)** Viral RNA level at 48 hr is graphed as fold change from level post-inoculation (t=1hr). *$p<0.01$ **(C-F)** Primary nasal or bronchial cells were transfected with SLR14-488 using lipofectamine as in Fig 1. Following transfection, cells were either collected within 1 hr for flow cytometry or incubated for 5 hr at 37°C, then cells were collected for RNA isolation and RT-qPCR to assess ISG induction. **(C)** Bars show mean fluorescence intensity in FL1 channel of untransfected cells (mock) or cells transfected with SLR14-488. Mean and S.D. of three replicates are shown. Autofluorescence of untreated nasal cells in FL1 channel was higher than that of bronchial cells (*$p<0.001$), but upon SLR14-488 transfection, fluroescence increased in all cells and cell types did not significantly differ in MFI. (**D**) Plot of representative samples from **(C)** showing distribution of cells in FL1 channel. **(E,F)** Level of IFNλ1 and IFIT2 mRNA in nasal and bronchial cells 5 hr post transfection with SLR14-488, normalized to HPRT and expressed as fold change from mock-treated bronchial cells. Significant difference was seen in mRNA level of IFNλ1 and IFIT2 in SLR14-488 transfected nasal and bronchial cells ($p<0.05$.) Results are representative of at least three independent experiments with at least two different donors for each cell type. Bars show mean and S.D. of 2-3 replicates per condition.

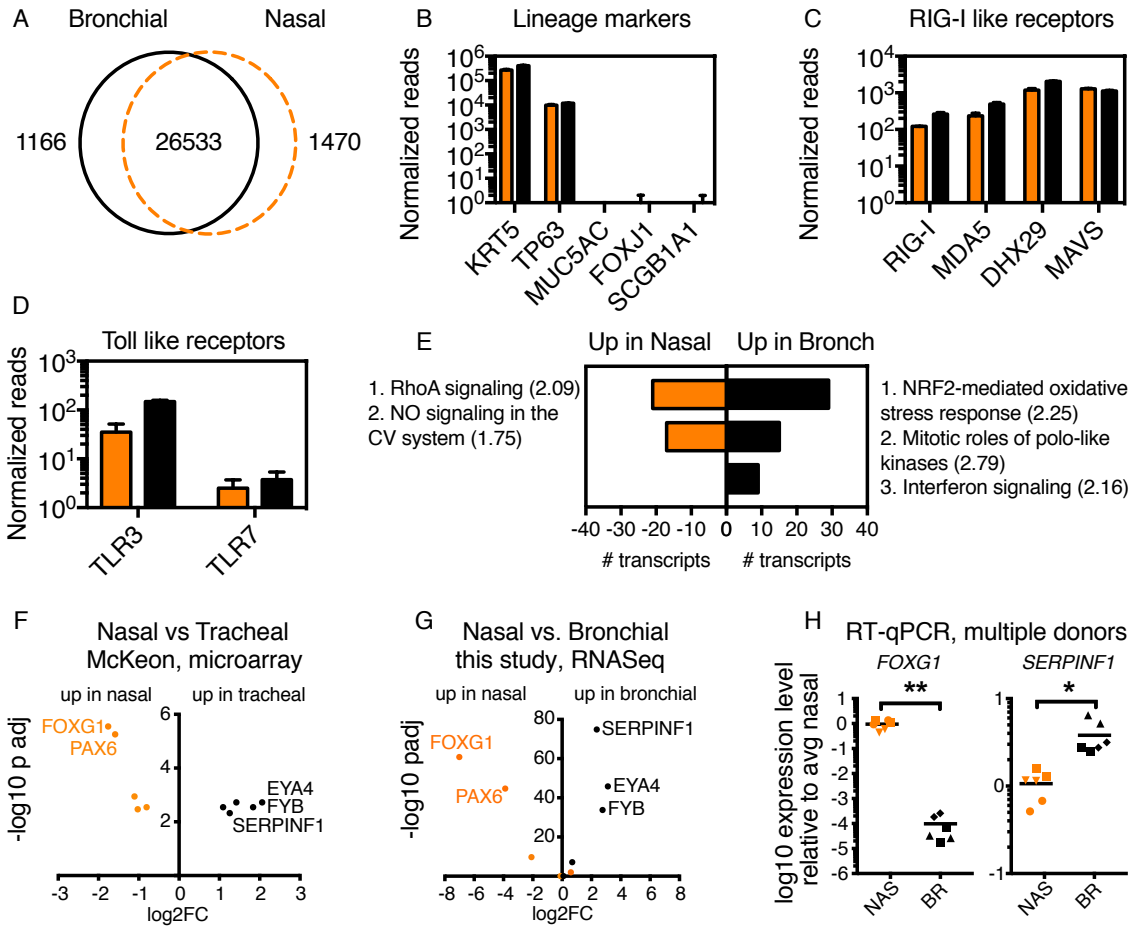

Fig. S2. ***Related to Figure 2.*** **Comparison of mRNA expression in resting bronchial and nasal primary airway epithelial cells (AECs).**

(**A**) Venn diagram showing number of transcripts in common and differentially enriched (log2FC>1 or log2FC<-1, P_{adj}<0.05) in resting bronchial vs. nasal epithelial cells.

(**B**) Relative expression level of lineage markers of basal cells (KRT5, TP63), goblet cells (MUC5AC), ciliated cells (FOXJ1), and Club cells (SCGB1A1.)

(**C**) Relative expression of mRNAs encoding components of RLR signaling pathways in resting AECs.

(**D**) Relative expression of TLRs involved in viral RNA recognition in AECs.

(**E**) Ingenuity Pathway analysis of pathways enriched in each cell type at rest. Only significantly differentially enriched pathways (Z score >1, p<0.01) are shown. Bars indicate number of differentially expressed transcripts associated with each pathway. Numbers in parentheses represent $-LOG_{10}$ p-value for relative enrichment of transcriptome for transcripts associated with the indicated Ingenuity pathway. Note that pathways associated with transcriptome changes following SLR14 treatment (Fig 2) are associated with much more significant p values.

(**F**) Volcano plot of microarray data from Kumar et al comparing nasal and tracheal airway progenitor cells, GSE32606. We compared all nasal sets to all tracheal data sets (2D and 3D growth conditions) and selected the 10 transcripts with highest differential expression by p-value.

(**G**) Volcano plot of RNAseq data from experiment shown in Fig 2, displaying top 10 transcripts differentially expressed in nasal vs. tracheal airway stem cells from Kumar et al identified in (F). Transcripts enriched in nasal vs. tracheal-derived cells in GSE32606 are indicated with orange dots.

(**H**) RT-qPCR data showing relative expression of FOXG1 and SERPINF1 mRNAs in cells from different donors used in this study. Plots show three donors per cell type with two replicates per donor (samples from different donors indicated by different symbols.) Expression level was calculated as ΔΔCt relative to ß-actin mRNA level in each sample, and is graphed as fold change from the average expression level in nasal-derived cells. *p<0.005, **p<0.0001

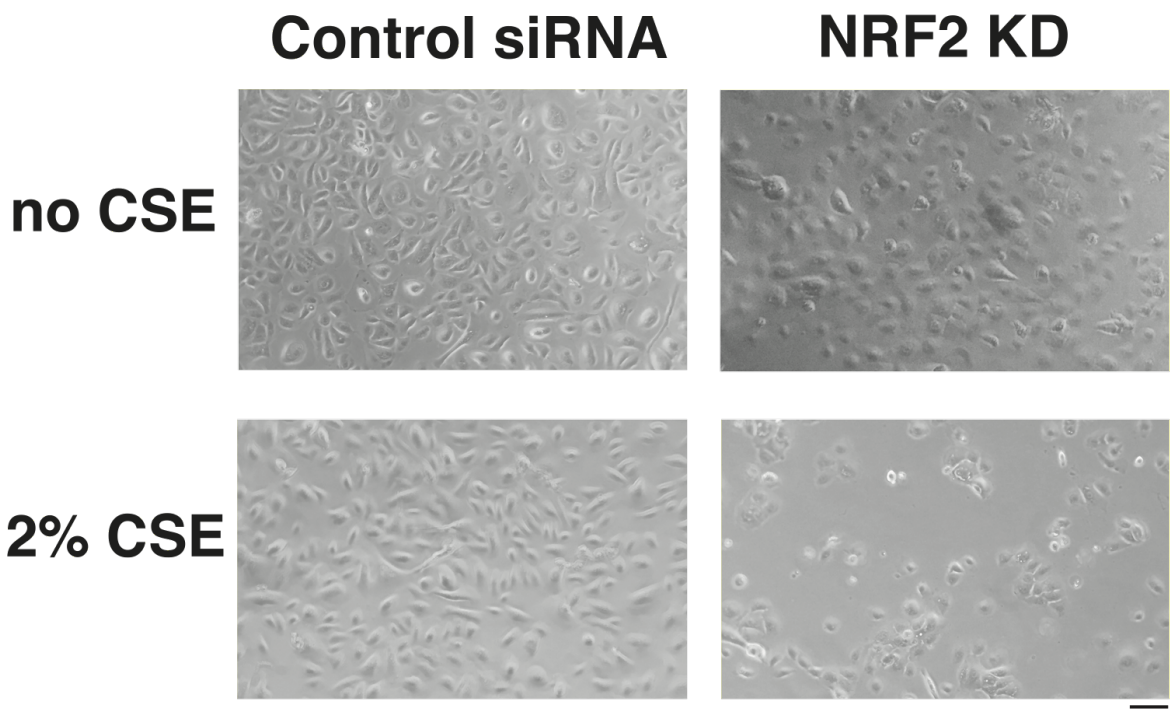

Fig S3. ***Related to Figure 4.*** **Micrographs showing nasal epithelial cells with or without NRF2 knockdown following exposure to CSE.** Nasal epithelial cells were treated with control RISC-free siRNA (left panels) or siRNA targeting NRF2 (right panels) and allowed to recover for 48 hr. Next, cells were incubated with medium only (top panels) or medium containing 2% CSE, followed by an additional 48 hr incubation. Cells treated with control siRNA maintained a healthy monolayer following exposure to 2% cigarette smoke extract (lower left panel) but NRF2 knockdown cells did not (lower right panel). Bar=100μm

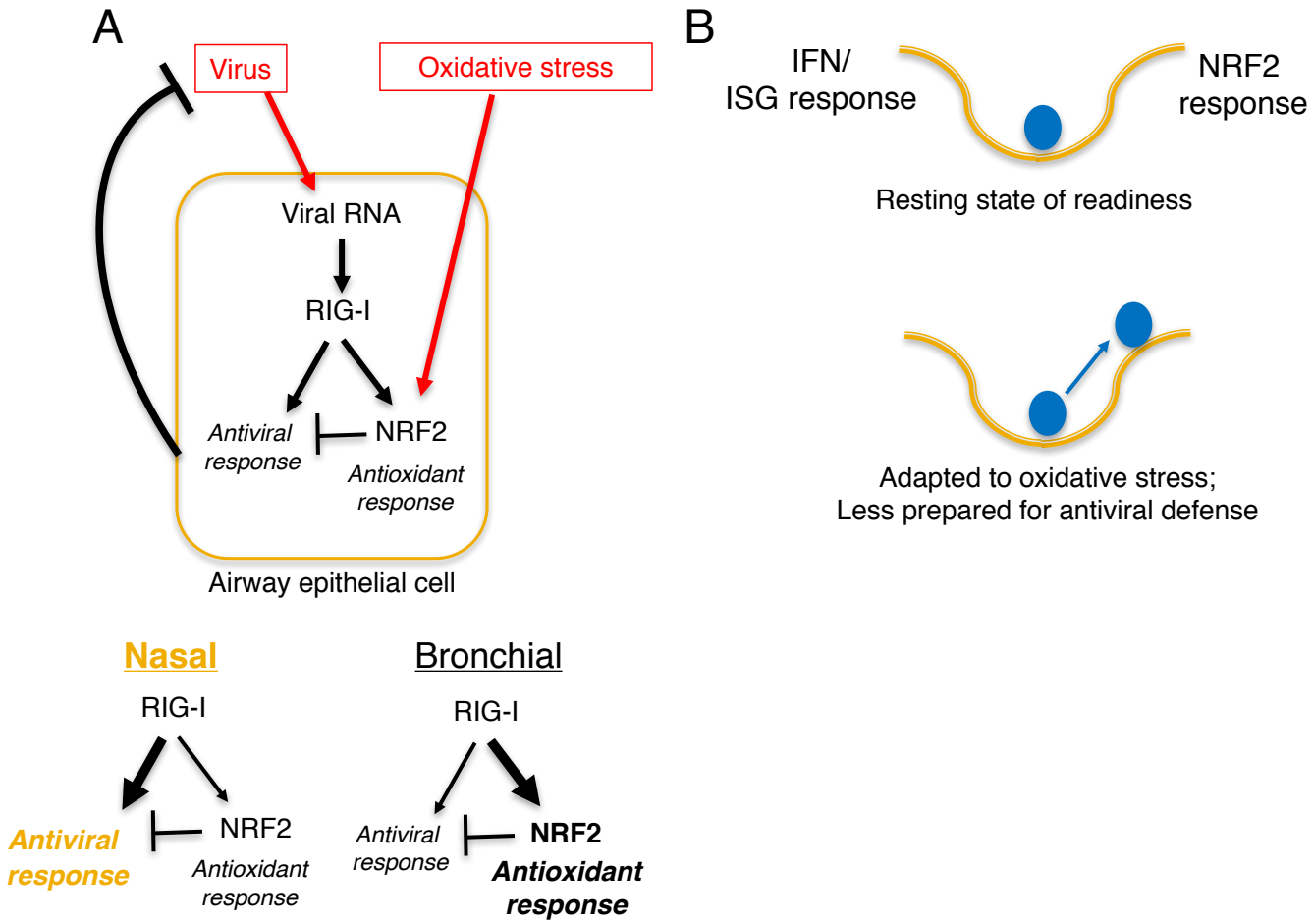

Fig S4. ***Related to Figures 3 & 4*****. Model for fine-tuning of airway defense showing tradeoff between NRF2 response and antiviral response.** Our data supports a model in which viral infection triggers two host protective responses, cell-intrinsic antiviral responses and the NRF2 mediated defense response. (**A**) Drawing shows signaling within an airway epithelial cell, showing the balance between these defense responses. Cell intrinsic differences shift the balance away from NRF2 activity in favor of antiviral defense in nasal cells, whereas bronchial cells show a cell-intrinsic bias favoring antioxidant defense. This difference in set-point between nasal and bronchial-derived airway epithelial cells may reflect the need for adaptations to counter the attenuating effects of cooler temperature in the nasal passages on antiviral defense. Current or recent exposure to environmental sources of oxidative stress (i.e. cigarette smoke) would be expected to enhance NRF2 activity and antioxidant defense at the expense of antiviral responses. (**B**) Line represents adaptive landscape in which resting cells are equally able to adapt to oxidative stress (with NRF2 response) or viral infection (with IFN response), however adaptation to oxidative stress creates biological state less able to adapt to viral infection (right panel.)

Table S1. *Related to Figure 2*. Ingenuity pathway analysis and pathway-associated transcripts, response to SLR14 in primary airway cells p<0.01, Z-score>1

Nasal

Ingenuity Canonical Pathways	-LOG p value	ratio	Zscore	Molecules
Interferon Signaling	13.3	4.17 E-01	3.207	IFIT3,SOCS1,OAS1,MX1,IFI35,IRF9,IFITM2,TAP1,IRF1,ISG15,IFITM3,IFIT1,IFI6,STAT1, IFITM1
Activation of IRF by Cytosolic Pattern Recognition Receptors	8.38	2.26 E-01	2.138	DHX58,ZBP1,IRF9,IL6,NFKB2,ISG15,IFIH1,IRF7,NFKBIA,JUN,DDX58,IFIT2,STAT1,TNF
Toll-like Receptor Signaling	7.33	1.89 E-01	2.714	TLR2,IL36G,JUN,NFKBIA,TICAM1,IL36RN,TNFAIP3,MAP2K3,EIF2AK2,IRAK3,NFKB2, UBC,TNF,IRAK2
Role of Pattern Recognition Receptors in Recognition of Bacteria and Viruses	7.3	1.44 E-01	3.317	PTX3,CXCL8,OAS1,LIF,PRKCQ,OAS2,IL6,NFKB2,OAS3,TLR2,IFIH1,NOD2,IRF7,TICAM1, DDX58,TGFB2,EIF2AK2,TNF
NRF2-mediated Oxidative Stress Response	6.78	1.17 E-01	2.887	PRKCQ,DNAJB4,NQO1,HSPB8,DNAJA4,HERPUD1,DNAJC3,GCLC,DNAJA1,DNAJB9,MAFF,TXNRD1,HMOX1,JUN,STIP1,MAP2K3,FOSL1,DNAJB1,GCLM,EIF2AK3,ENC1
p38 MAPK Signaling	6.24	1.37 E-01	1.807	TP53,PLA2G3,IRAK3,MKNK2,CREB5,CDC25B,PLA2G4E,PLA2G4A,IL36G,DUSP1,IL36RN,TGFB2,MAP2K3,STAT1,TNF,IRAK2
Hypoxia Signaling in the Cardiovascular System	5.39	1.69 E-01	2.236	TP53,HSP90B1,JUN,NFKBIA,EDN1,HSP90AB1,NQO1,HSP90AA1,CREB5,UBE2L6, UBE2D3
MIF Regulation of Innate Immunity	4.54	1.95 E-01	2.828	TP53,PLA2G4E,PLA2G4A,JUN,NFKBIA,PLA2G3,PTGS2,NFKB2
iNOS Signaling	4.3	1.82 E-01	2.449	CAMK4,JUN,NFKBIA,NFKB2,IRAK3,STAT1,IRF1,IRAK2
TREM1 Signaling	4.03	1.33 E-01	3.162	TLR2,CXCL8,NLRC5,CXCL3,NOD2,ICAM1,NLRP10,NFKB2,IL6,TNF
Death Receptor Signaling	3.94	1.2E-01	1.508	NFKBIA,PARP10,ZC3HAV1,TNFSF10,PARP12,NFKB2,CFLAR,BIRC3,TNF,PARP9, PARP14
Role of IL-17F in Allergic Inflammatory Airway Diseases	3.46	1.59 E-01	2.449	CXCL10,CXCL8,MMP13,CXCL1,NFKB2,IL6,CREB5
MIF-mediated Glucocorticoid Regulation	3.35	1.82 E-01	2.236	PLA2G4E,PLA2G4A,NFKBIA,PLA2G3,PTGS2,NFKB2
Retinoic acid Mediated Apoptosis Signaling	3.28	1.31 E-01	2.121	PARP10,ZC3HAV1,TNFSF10,PARP12,CFLAR,PARP9,IRF1,PARP14
Eicosanoid Signaling	3.14	1.25 E-01	2.449	PLA2G4E,PLA2G4A,ABHD3,PLA2G3,RARRES3,PNPLA3,PTGS2,PTGER4
IL-6 Signaling	3.06	9.48 E-02	2.111	CXCL8,SOCS1,SOCS3,IL36G,JUN,NFKBIA,IL36RN,MAP2K3,NFKB2,IL6,TNF
Mitotic Roles of Polo-Like Kinase	3.05	1.21 E-01	1.342	CDC25B,HSP90B1,ESPL1,CDC20,HSP90AB1,HSP90AA1,CDC25A,CCNB1

Dendritic Cell Maturation	2.94	7.91 E-02	3.051	TLR2,B2M,IL36G,NFKBIA,ICAM1,DDR2,RELB,IL36RN,IL6,NFKB2,STAT1,CREB5,TNF,FCGR1B
PI3K/AKT Signaling	2.85	8.94 E-02	2.333	TP53,HSP90B1,NFKBIA,HSP90AB1,GDF15,ITGA2,HSP90AA1,PTGS2,NFKB2,SFN,INPP5D
PI3K Signaling in B Lymphocytes	2.74	8.66 E-02	2.530	CAMK4,JUN,ATF3,NFKBIA,DAPP1,LYN,NFATC2,NFATC4,PLEKHA4,NFKB2,INPP5D
Role of RIG1-like Receptors in Antiviral Innate Immunity	2.73	1.4E-01	1.342	DHX58,IFIH1,IRF7,NFKBIA,DDX58,NFKB2
Acute Phase Response Signaling	2.66	7.69 E-02	2.111	HMOX1,SOCS3,SOCS1,IL36G,JUN,NFKBIA,IL36RN,CFB,VWF,MAP2K3,IL6,NFKB2,TNF
Endothelin-1 Signaling	2.6	7.56 E-02	2.496	PLA2G4E,HMOX1,PLA2G4A,JUN,PRKCQ,EDN1,ABHD3,MAPK15,SHC2,PLA2G3,RARRES3,PNPLA3,PTGS2
NF-κB Signaling	2.6	7.56 E-02	1.941	TLR2,IL36G,NFKBIA,PRKCQ,BMP2,RELB,IL36RN,PELI1,TNFAIP3,EIF2AK2,IRAK3,NFKB2,TNF
B Cell Receptor Signaling	2.55	7.47 E-02	3.051	CAMK4,JUN,PRKCQ,NFKBIA,DAPP1,PAG1,LYN,NFATC2,MAP2K3,NFATC4,NFKB2,CREB5,INPP5D
TNFR1 Signaling	2.43	1.22 E-01	1.342	JUN,NFKBIA,TNFAIP3,NFKB2,BIRC3,TNF
HMGB1 Signaling	2.41	8.33 E-02	2.530	CXCL8,ICAM1,JUN,LIF,TGFB2,MAP2K3,NFKB2,IL6,TNF,PLAT
UVA-Induced MAPK Signaling	2.25	9.09 E-02	1.890	TP53,JUN,PARP10,ZC3HAV1,PARP12,STAT1,PARP9,PARP14
Colorectal Cancer Metastasis Signaling	2.2	6.36 E-02	3.742	TP53,MMP13,VEGFC,NFKB2,IL6,TLR2,FZD4,JUN,TGFB2,PTGS2,GNB1L,STAT1,TNF,MMP1,PTGER4
Gαs Signaling	2.2	8.26 E-02	2.121	HCAR3,RGS2,RAPGEF2,RAPGEF3,GNB1L,CREB5,HCAR2,PTGER4,ADRB2
Phospholipase C Signaling	2.18	6.33 E-02	2.887	CAMK4,PRKCQ,ITGA2,PLA2G3,RAPGEF3,NFATC4,NFKB2,CREB5,TGM2,PLA2G4E,HMOX1,PLA2G4A,LYN,NFATC2,GNB1L
Type I Diabetes Mellitus Signaling	2.17	8.18 E-02	1.414	SOCS1,SOCS3,NFKBIA,MAP2K3,NFKB2,HLA-F,STAT1,TNF,IRF1

Antioxidant Action of Vitamin C	4.99	1.31 E-01	-3.162	PLA2G4E,HMOX1,PLA2G4A,NFKBIA,ABHD3,PLA2G3,RARRES3,PNPLA3,NFKB2,SLC23A3,GLRX,TNF,TXNRD1
PPAR Signaling	4.57	1.29 E-01	-3.464	HSP90B1,IL36G,JUN,NFKBIA,HSP90AB1,PPARD,IL36RN,HSP90AA1,PTGS2,NFKB2,TNF,PPARGC1A
LXR/RXR Activation	3.46	9.92 E-02	-1.414	APOL1,FDFT1,IL36G,LDLR,FASN,IL36RN,PTGS2,NFKB2,IL6,HMGCR,TNF,CYP51A1
PPARα/RXRα Activation	2.05	6.74 E-02	-1.265	HSP90B1,JUN,NFKBIA,HSP90AB1,HELZ2,FASN,TGFB2,HSP90AA1,MAP2K3,NFKB2,IL6,PPARGC1A

Bronchial

Ingenuity Canonical Pathways	-log(p-value)	Ratio	z-score	Molecules
NRF2-mediated Oxidative Stress Response	11.8	1.06 E-01	2.333	DNAJB4,NQO1,DNAJA4,HSPB8,HERPUD1,DNAJC3,GCLC,DNAJA1,DNAJB9,TXNRD1,MAFG,HMOX1,FOS,DNAJB11,SQSTM1,DNAJB1,GCLM,EIF2AK3,ENC1
Interferon Signaling	6.53	1.94 E-01	1.890	IFIT3,SOCS1,IFIT1,OAS1,MX1,IRF1,ISG15
Role of Pattern Recognition Receptors in Recognition of Bacteria and Viruses	5.36	8E-02	1.633	IFIH1,CXCL8,OAS1,IRF7,NOD2,OAS2,DDX58,IL1B,IL6,OAS3
Activation of IRF by Cytosolic Pattern Recognition Receptors	3.88	9.68 E-02	1.633	IFIH1,IRF7,DDX58,IL6,IFIT2,ISG15
eNOS Signaling	3.34	5.63 E-02	-2.000	HSPA8,HSP90B1,AQP5,CCNA1,HSPA1A/HSPA1B,HSPA6,HSP90AA1,HSPA5
PPAR Signaling	3.75	7.53 E-02	-1.134	IL33,FOS,HSP90B1,IL36G,HSP90AA1,IL1B,PTGS2
Antioxidant Action of Vitamin C	2.79	6.06 E-02	-1.000	HMOX1,ABHD3,PLA2G3,PLCH2,GLRX,TXNRD1

Table S2. *Related to key resources table*. qPCR primers used in this study

REAGENT or RESOURCE	SOURCE	IDENTIFIER
Oligonucleotides		
b-actin, F:CCTGGCACCCAGCACAAT	Keck DNA synthesis facility, Yale	n/a
b-actin, R:GCCGATCCACACGGAGTACT	Keck DNA synthesis facility, Yale	n/a
IFN lambda 1, F:GACTTTGGTGCTAGGCTTGG	Keck DNA synthesis facility, Yale	n/a
IFN lambda 1, R:AGATTTGAACCTGCCAATGTG	Keck DNA synthesis facility, Yale	n/a
IFN beta, F: CTTTCGAAGCCTTTGCTCTG	Keck DNA synthesis facility, Yale	n/a
IFN beta, R: GGAGAGCAATTTGGAGGAGAC	Keck DNA synthesis facility, Yale	n/a
OAS1, F:GCTCCTACCCTGTGTGTGTGT	Keck DNA synthesis facility, Yale	n/a
OAS1, R: : TGGTGAGAGGACTGAGGAAGA	Keck DNA synthesis facility, Yale	n/a
IFIT2, F: CCTCAAAGGGCAAAACGAGG	Keck DNA synthesis facility, Yale	n/a
IFIT2, R: CTGATTTCTGCCTGGTCAGC	Keck DNA synthesis facility, Yale	n/a
NRF2, F: TTCTGACTCCGGCATTTCAC	Keck DNA synthesis facility, Yale	n/a
NRF2, R: AGGCCAAGTAGTGTGTCTCC	Keck DNA synthesis facility, Yale	n/a
NQO1, F: GGACGTCCTTCAACTATGCC	Keck DNA synthesis facility, Yale	n/a
NQO1, R: TCATGGCATAGAGGTCCGAC	Keck DNA synthesis facility, Yale	n/a
GCLC, F: CAAACCCAAACCATCCTACCC	Keck DNA synthesis facility, Yale	n/a
GCLC, R: ACTCGGACATTGTTCCTCCG	Keck DNA synthesis facility, Yale	n/a
MAVS, F: GCAGCTCTGAGAATAGGGGC	Keck DNA synthesis facility, Yale	n/a
MAVS, R: TGGCAAGATCCTCGAAGCAG	Keck DNA synthesis facility, Yale	n/a
FOXG1, F: GCCAGCAGCACTTTGAGTTAC	Keck DNA synthesis facility, Yale	n/a
FOXG1, R: CCCAGCGAGTTCTGAGTCAA	Keck DNA synthesis facility, Yale	n/a
SERPINF1, F: TTACGCTATGGCTTGGATTC	Keck DNA synthesis facility, Yale	n/a
SERPINF1, R: AAATTCTGGGTCACTTTCAGG	Keck DNA synthesis facility, Yale	n/a
RV1B, 5'UTR, F: ACGGACACCCAAAGTAGTCG	Keck DNA synthesis facility, Yale	n/a
RV1B, 5'UTR, R: ATCTTTGGTTGGTCGCTCAG	Keck DNA synthesis facility, Yale	n/a